

1 **Supplementary Information for**

2
3 **Photodissociation of particulate nitrate as a source of daytime tropospheric Cl₂**

4
5 Xiang Peng^{1,2}, Tao Wang^{1*}, Weihao Wang^{1,3}, A.R. Ravishankara⁴, Christian George⁵,
6 Men Xia¹, Min Cai⁶, Qinyi Li⁷, Christian Mark Salvador^{8,15}, Chiho Lau⁹, Xiaopu Lyu¹,
7 Chun Nan Poon¹, Abdelwahid Mellouki⁶, Yujing Mu¹⁰, Mattias Hallquist⁸, Alfonso
8 Saiz-Lopez⁷, Hai Guo¹, Hartmut Herrmann^{11,12}, Chuan Yu^{1,13}, Jianing Dai^{1,16}, Yanan
9 Wang¹, Xinke Wang⁵, Alfred Yu⁹, Kenneth Leung⁹, Shuncheng Lee¹, and Jianmin Chen¹⁴

10 *email: cetwang@polyu.edu.hk

11
12 Contents:

13 Supplementary Figures: Supplementary Fig. 1 to Supplementary Fig. 14

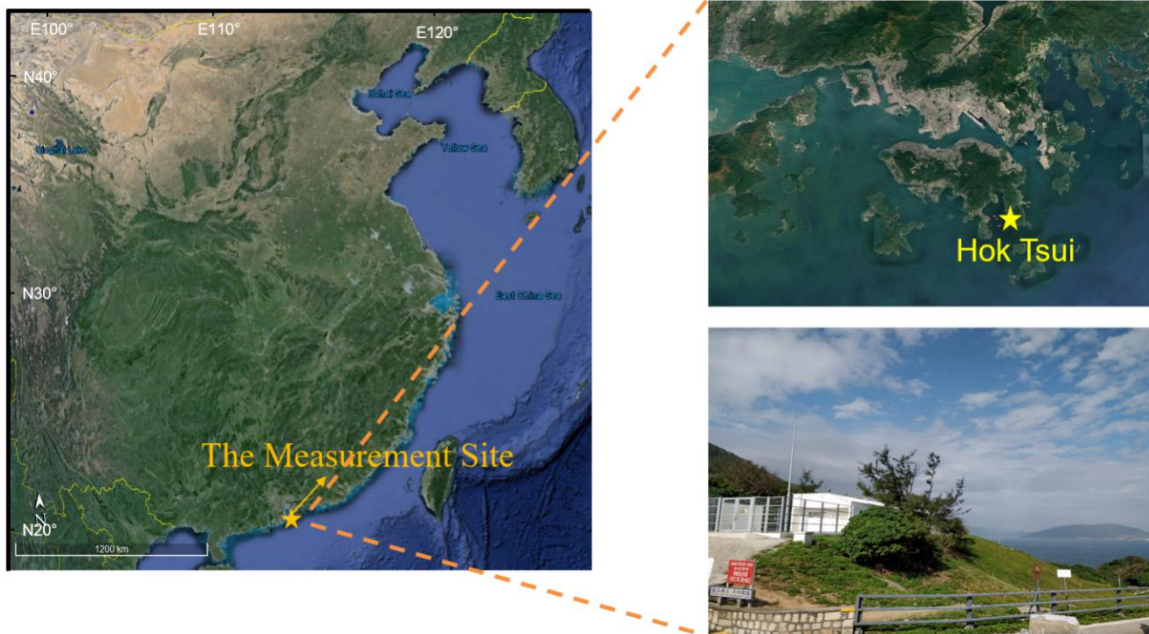
14 Supplementary Tables: Supplementary Table 1 to Supplementary Table 3

15 References

16

17 **Supplementary Figures:**

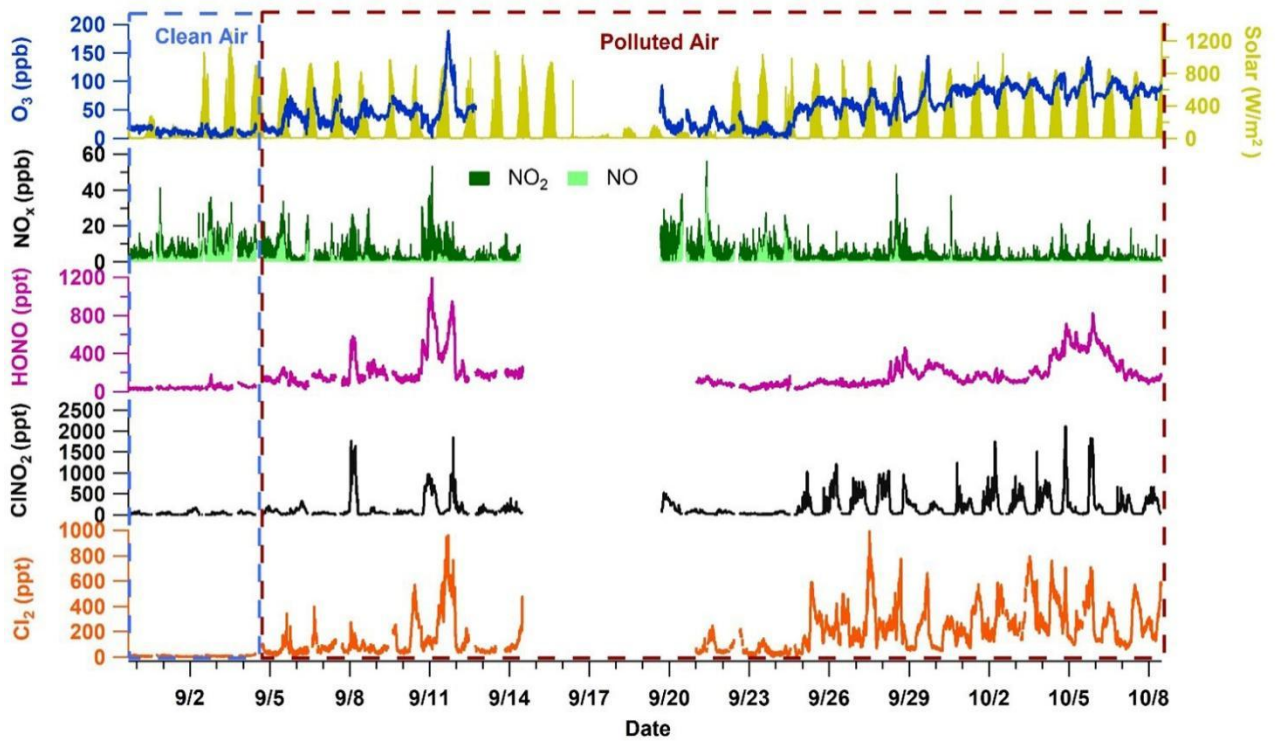
18 **Supplementary Fig. 1. The locations of the measurement site in Cape D’Aguilar**
19 **(also called Hok Tsui) in Hong Kong (yellow star). (Map credit: Google Earth)**



20

21

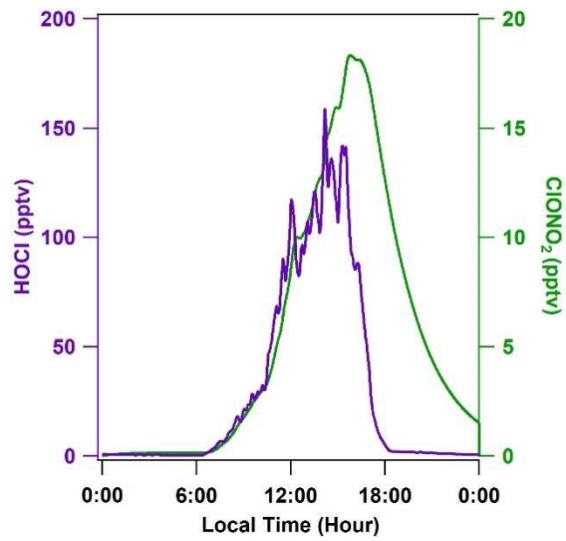
22 **Supplementary Fig. 2. Ambient observations from 31 August to 9 October of 2018 in**
23 **the clean air mass which originated from the ocean and in the polluted air mass**
24 **which originated from the continental region.** The measurements during 14-21
25 September were interrupted due to a super typhoon (Mangkhut) hitting the south China
26 coast (including Hong Kong).



27

28

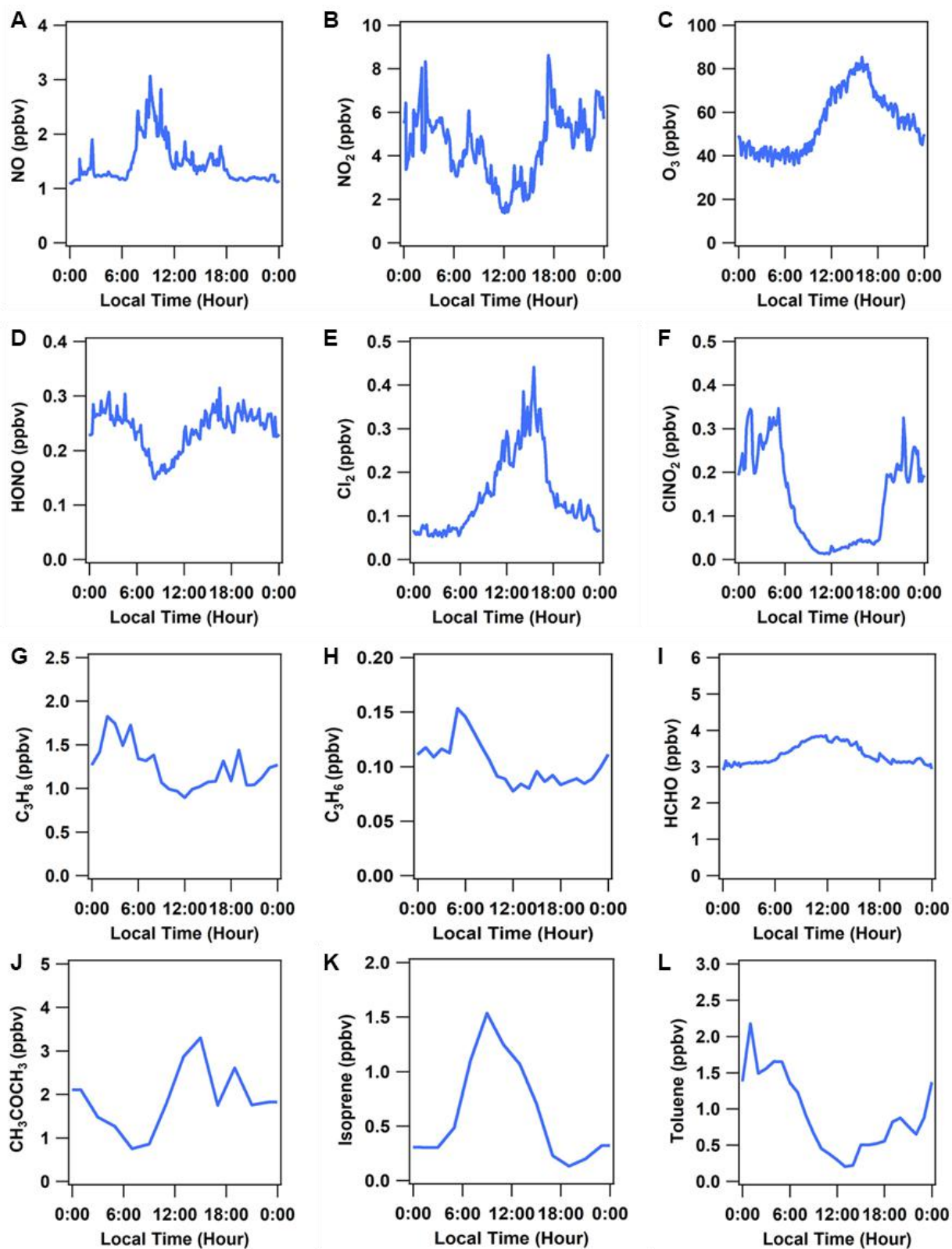
29 **Supplementary Fig. 3. The model predicted average diurnal profiles of HOCl and**
30 **ClONO₂ averaged for the period of 4 -14 September 2018.**



31

32

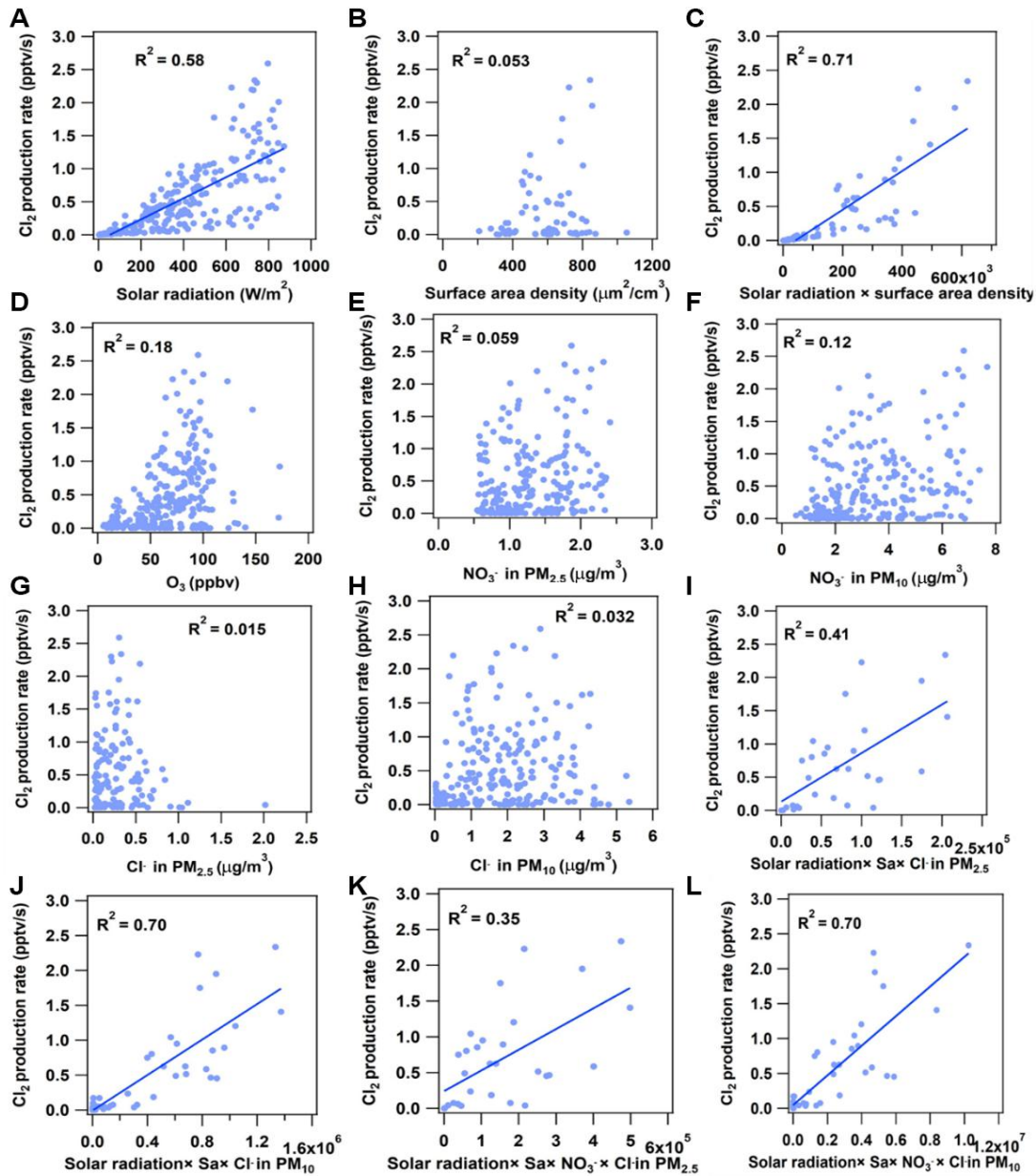
33 **Supplementary Fig. 4. Average diurnal profiles of select input parameters used in**
34 **the model simulation (4-14 September 2018).**



35

36

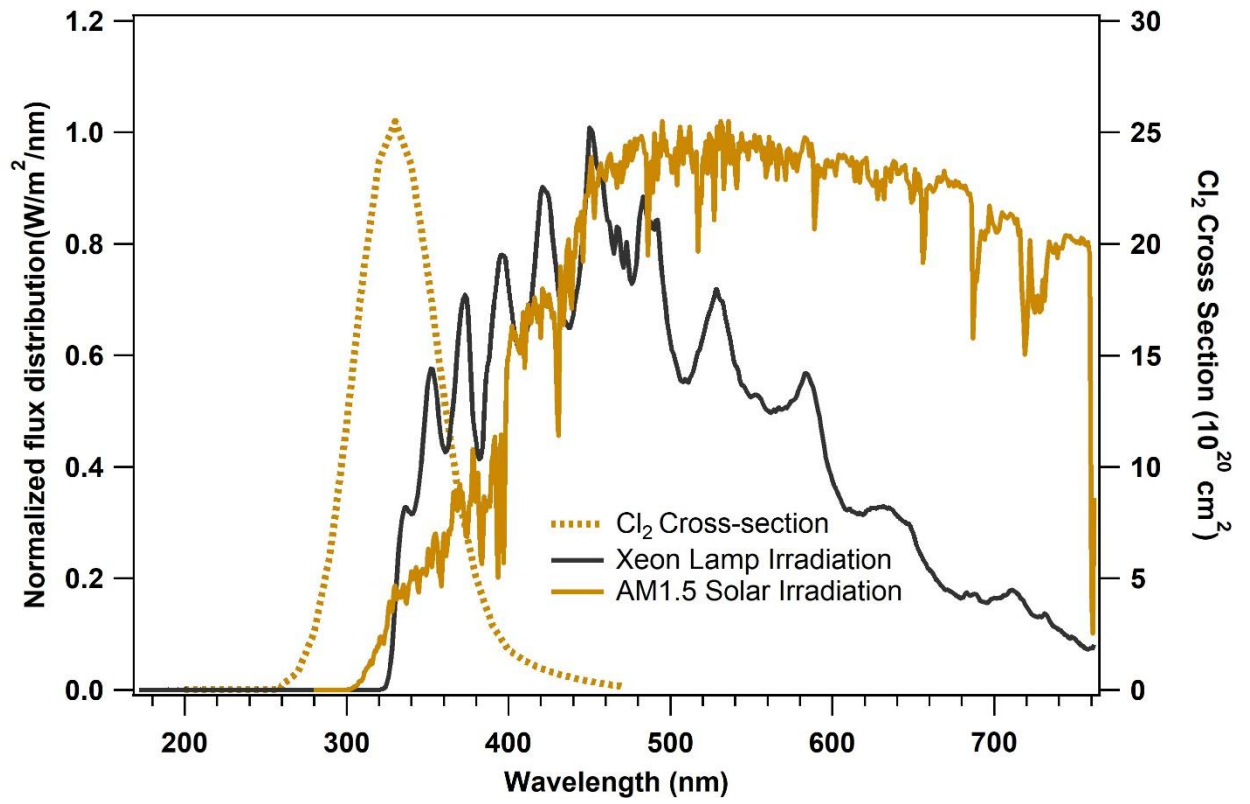
37 **Supplementary Fig. 5. Scatter plot of the production rate of Cl₂ (P_{Cl₂}) and various**
 38 **measured parameters from 08:00 to 18:00 in the continental air mass during 5**
 39 **September and 9 October 2018. The P_{Cl₂} equals the photolysis rate of Cl₂ (J_{Cl₂} ×**
 40 **measured Cl₂ concentration), assuming Cl₂ in a photo stationary state (given its short**
 41 **lifetime of ~7 minutes at noob in our study). J_{Cl₂} was calculated from the TUV model**
 42 **(http://cprm.acom.ucar.edu/Models/TUV/Interactive_TUV) under clear sky conditions**
 43 **and then scaled to the solar irradiation derived J_{NO₂} (see Methods section 3). The Sa**
 44 **represents the aerosol surface area density (μm² cm⁻³).**



45

46

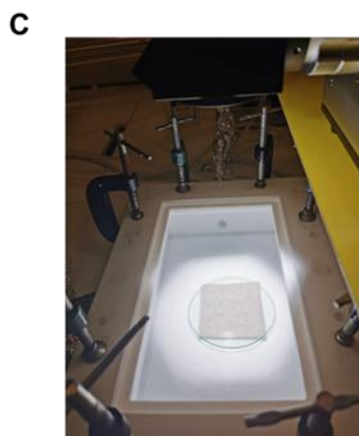
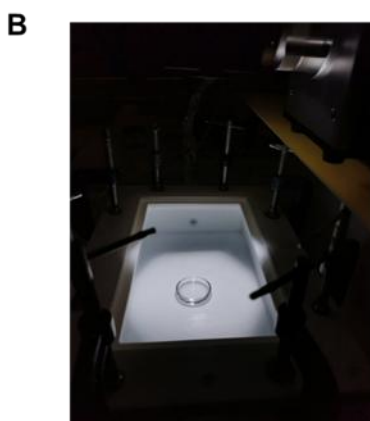
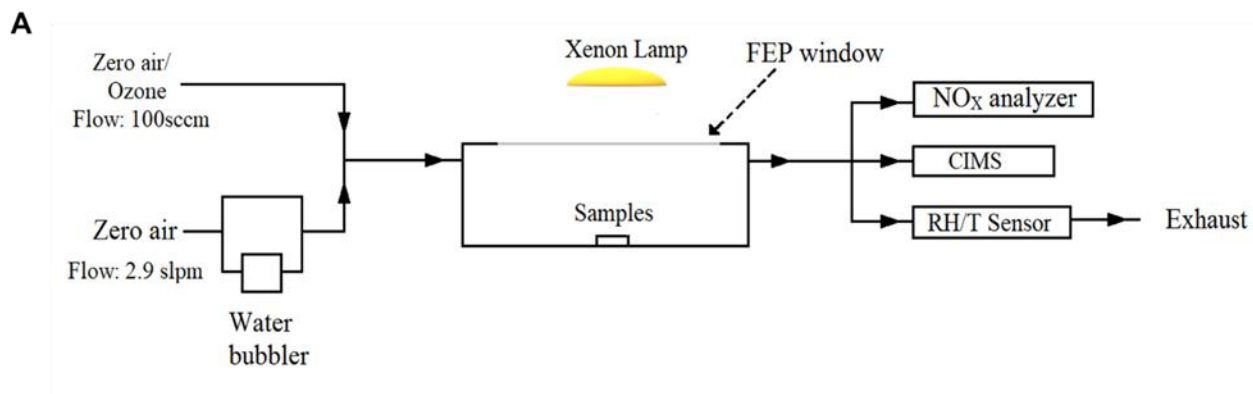
47 **Supplementary Fig. 6.** The irradiation spectrum of the xenon lamp used in this
48 study and the Cl₂ cross-section (IUPAC) (<http://iupac.pole-ether.fr/index.html>).



49

50

51 **Supplementary Fig. 7. The schematic and photos of the experimental apparatus for**
52 **Cl₂ production by irradiation.** The chamber is made of TFE Teflon (1.875L,
53 25cm-length × 15cm-width × 4cm-height) with a Teflon-film window on the top.

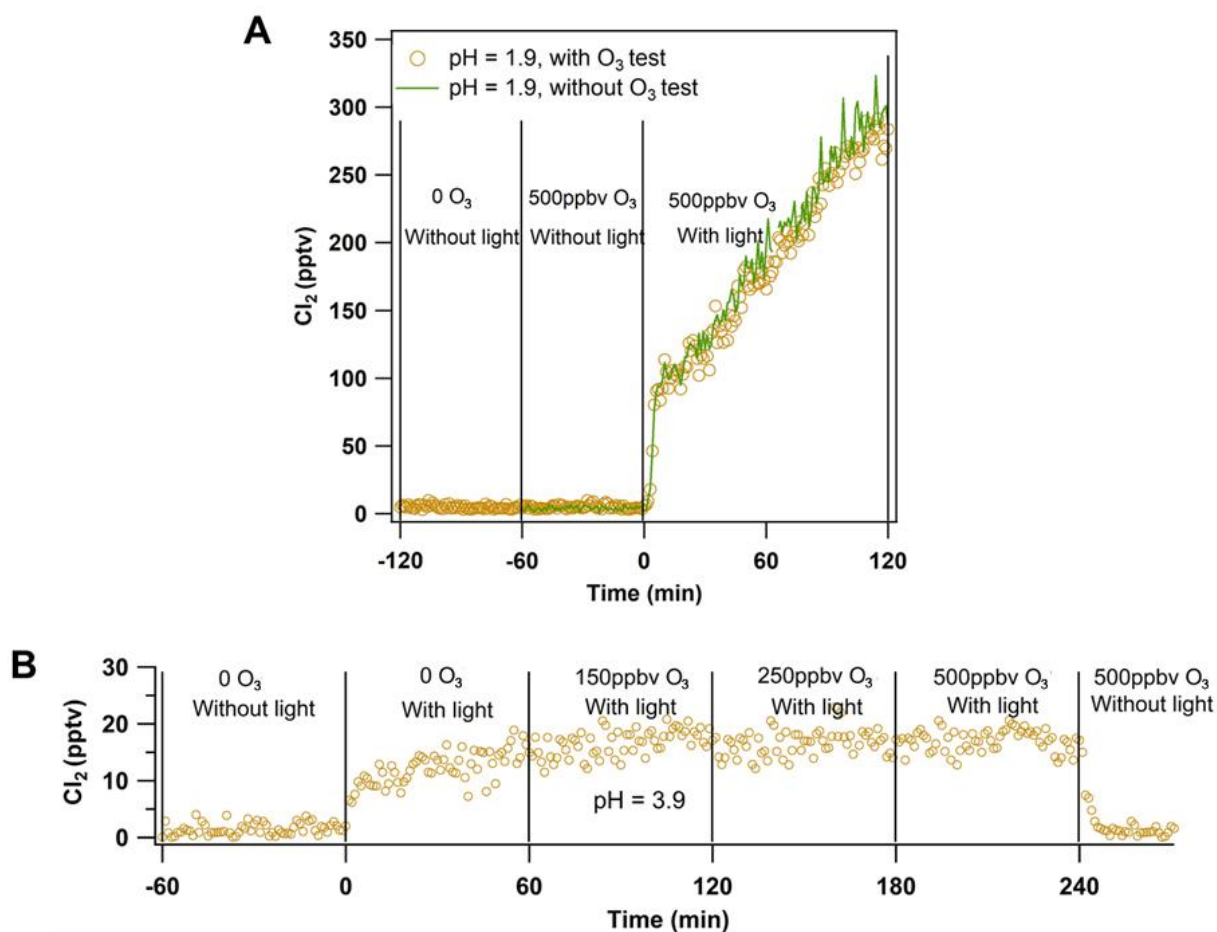


54

55

56 **Supplementary Fig. 8. Ozone experiment results on solutions.** (A) Comparison of
 57 1-min average Cl_2 mixing ratios without and with ozone. Acidic liquid solution samples
 58 (pH=1.9) were illuminated at $t=0$. The green line represents the result without ozone, and
 59 the orange cycle represents result with ozone. In the ozone test, about 500 ppbv ozone
 60 was added at $t=-60$ min. (B) Time series of Cl_2 mixing ratios with the addition of
 61 various levels of ozone. Liquid solution samples (pH=3.9) were illuminated at $t=0$. About
 62 150 ppbv ozone was added at $t=-60$ min., and the ozone level was changed to 250 ppbv
 63 at $t=120$, and further changed to 500 ppbv at $t=180$ min. The xenon lamp was turned off
 64 at $t=240$ min. Experimental conditions: 75-83% RH, 298 K in air, 15A Xenon Lamp, and
 65 one 4 ml liquid solution sample containing 1M NaCl + 1M NaNO₃.

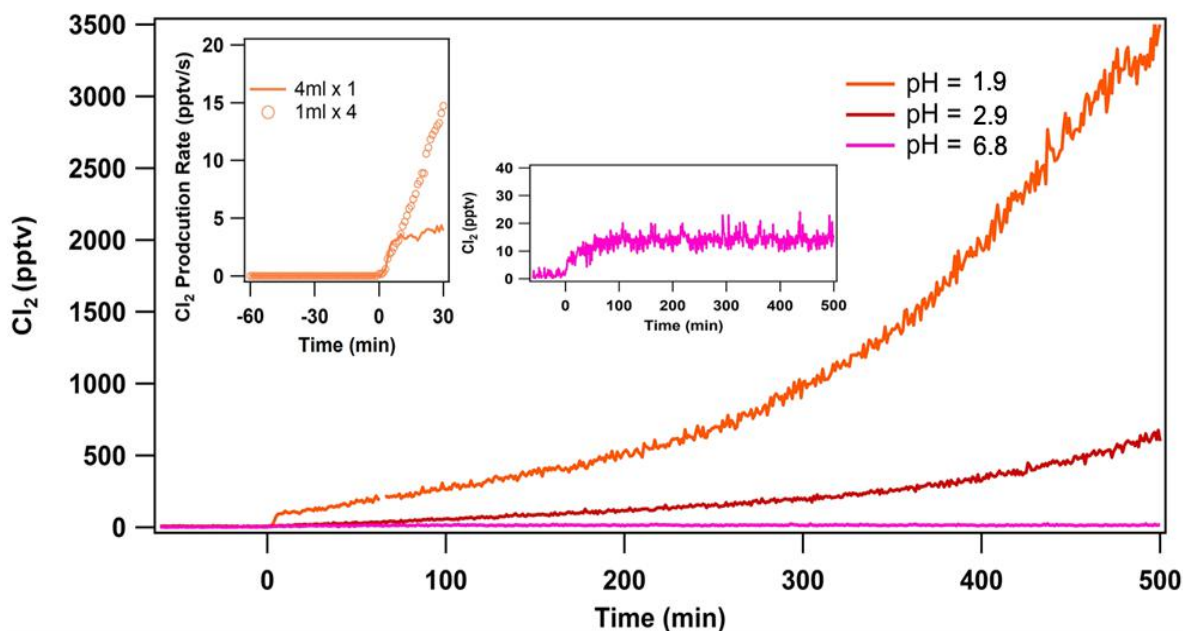
66



67

68

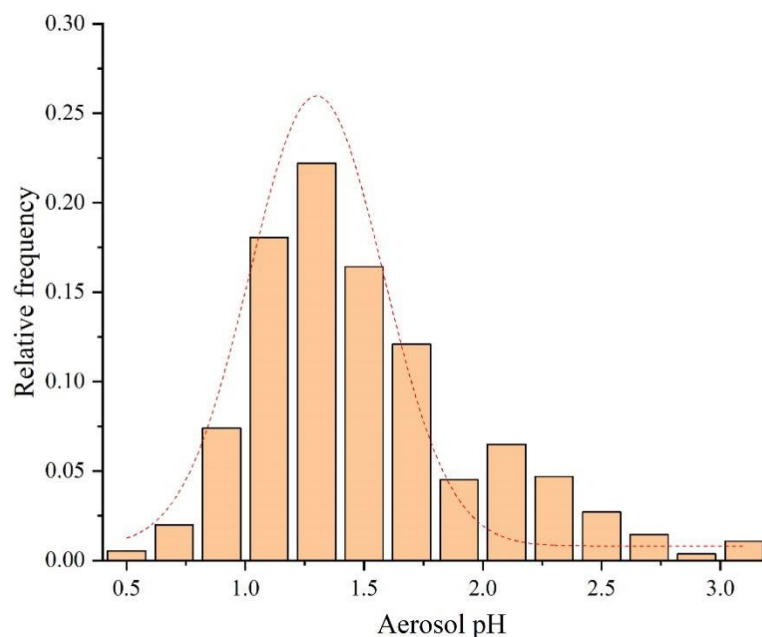
69 **Supplementary Fig. 9. Experimental results on solutions with different initial pH.**
70 Time series of 1-min average Cl_2 . Liquid solution samples (with the initial pH of 1.9,
71 2.9, and 6.8) were illuminated at $t=0$. The left insert: dependence of the Cl_2 yield (the
72 production of Cl_2) as a function of time under the initial $\text{pH}= 1.9$. The orange cycle
73 represents the use of one petri dish with 4ml solution, and the orange line represents the
74 use of four Petri dishes with 1ml solution per petri dish. The right insert: the enlarged
75 experimental results on solutions with the initial pH of 6.8. Experimental conditions:
76 75-83% RH, 298 K in air, 15A xenon lamp, and total 4 ml liquid solution containing 1M
77 $\text{NaCl} + 1\text{M NaNO}_3$.



78

79

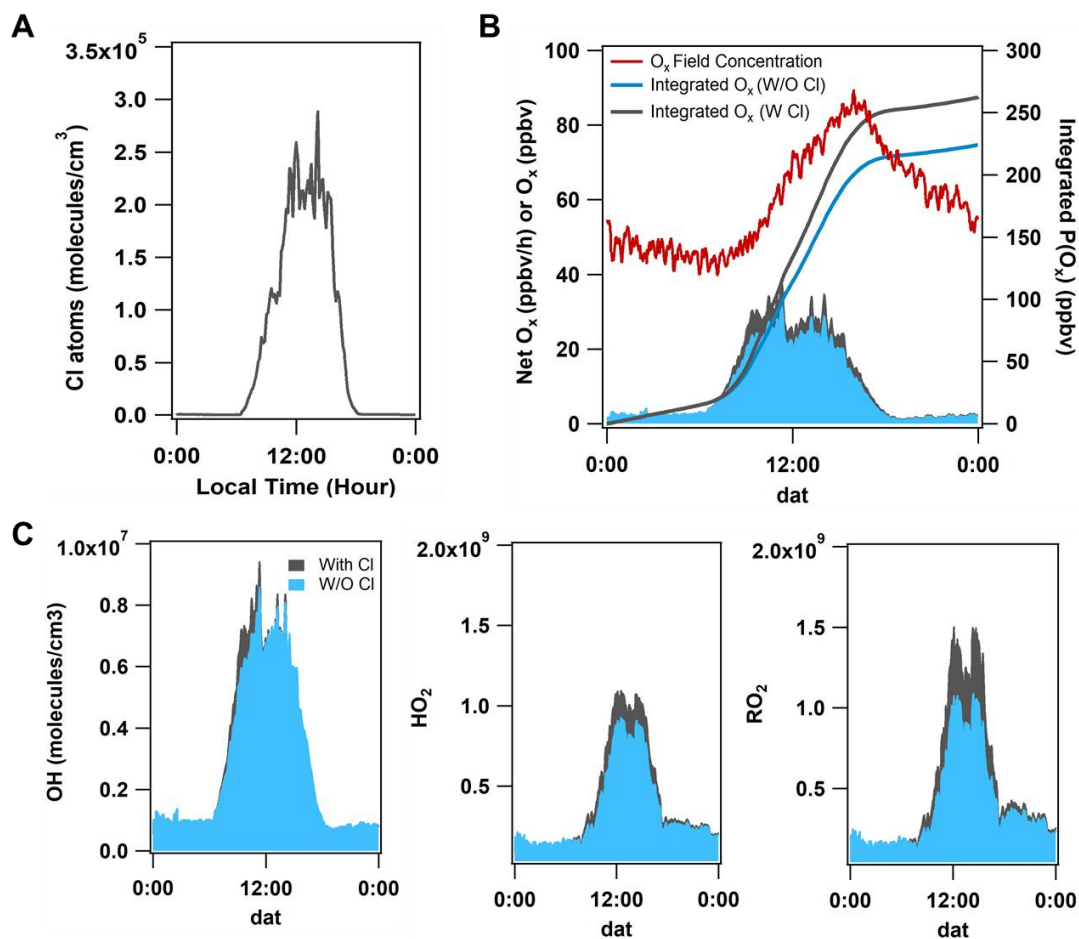
80 **Supplementary Fig. 10. Relative frequency distribution of E-AIM calculated pH of**
81 **hourly aerosol in PM_{2.5} during the Hok Tsui observation from 31 August to 9**
82 **October in 2018.** The number of data points is 555. The red dashed line represents a
83 regression of the pH by Gaussian distributions. Details of E-AIM model setup are as
84 follows. Model III with the batch mode was selected. The default temperature, pressure,
85 and volume were adopted as 298.15 K, 1 atm, and 1 m³, respectively. H⁺ was set to
86 balance the charges of anions and cations. Br⁻ and OH⁻ were set as zero. Water
87 dissociation is considered (parameter e=1). Gas-phase HNO₃, HCl, NH₃, and H₂SO₄ are
88 allowed and are partitioned between the gas phase and the condensed phases (parameter p,
89 q, r, s = 0). The model is configured to search all the possible solids (parameter u=0).
90 Organic compounds are not considered in the model. The E-AIM estimated average
91 equivalent Cl⁻ molarity in PM_{2.5} was 0.10 mol L⁻¹ (standard deviation: 0.19 mol L⁻¹) and
92 gas-phase HCl concentration was 0.96 ppbv (standard deviation: 0.52 ppbv).



93

94

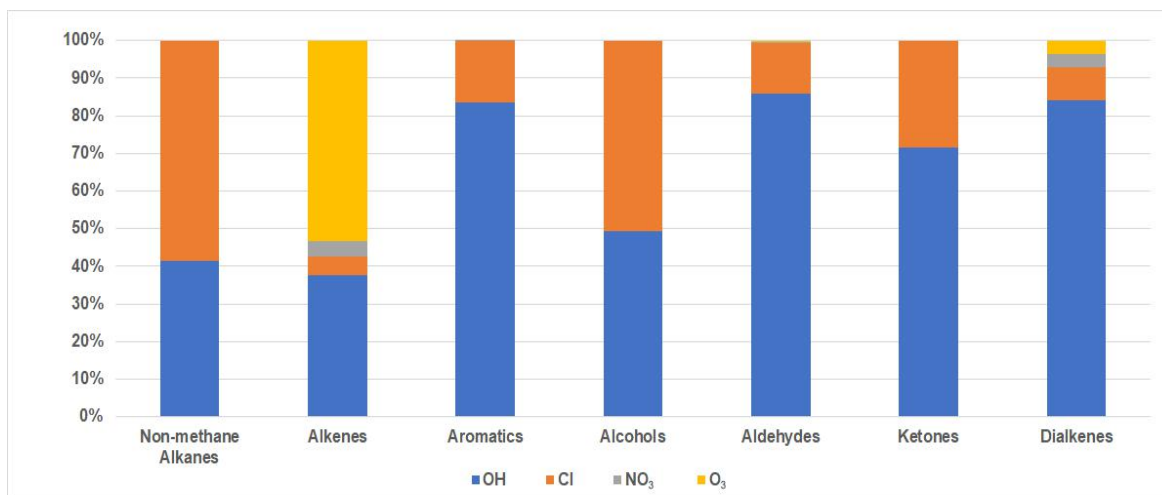
95 **Supplementary Fig. 11. The model calculated contributions of net ozone production**
 96 **rates and radical abundance averaged for the period of 4 -14 September 2018. (A)**
 97 **The average diurnal profiles of Cl atom concentrations. (B) The average diurnal profiles**
 98 **of the net production rate of O_x ($= O_3 + NO_2$) (different color bars). The blue bar and**
 99 **black bar represent results without Cl chemistry and with Cl chemistry, respectively. The**
 100 **red line represents field measurements of O_x . (C) The average diurnal profiles of OH,**
 101 **HO_2 , and RO_2 . The blue and black bars have the same meaning as panel (B).**



102

103

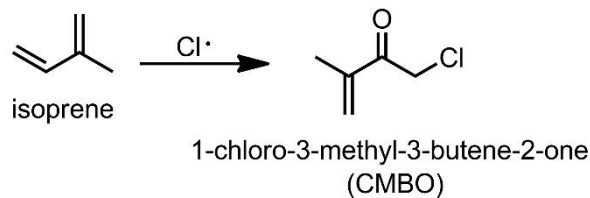
104 **Supplementary Fig. 12. Calculated hydrocarbon oxidation rates by different**
105 **oxidants.** Relative contributions to the daily integrated oxidation of alkanes, alkenes
106 (without dialkenes), aromatics, alcohols aldehyde, ketones, and dialkenes by OH, Cl,
107 NO₃, and O₃ (averaged for the time period of 4-14 September of 2018).



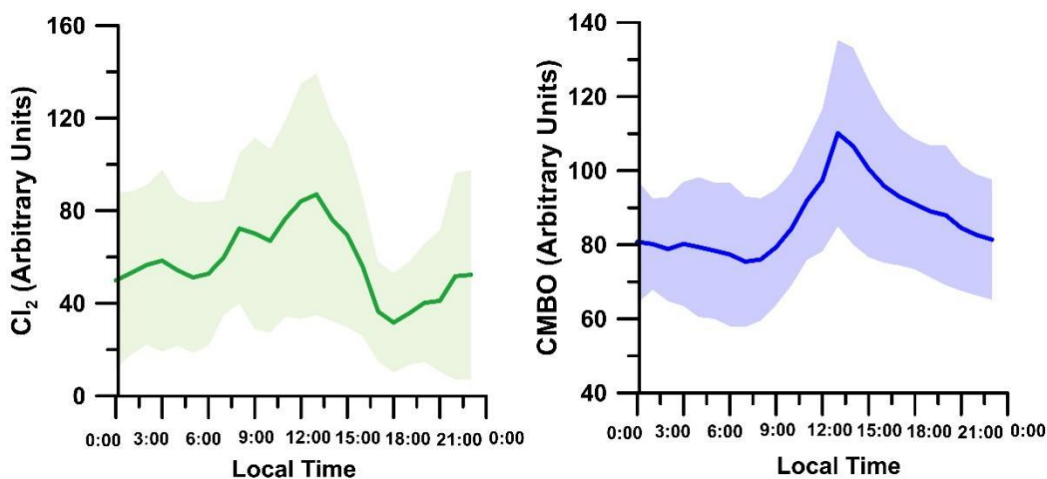
108

109

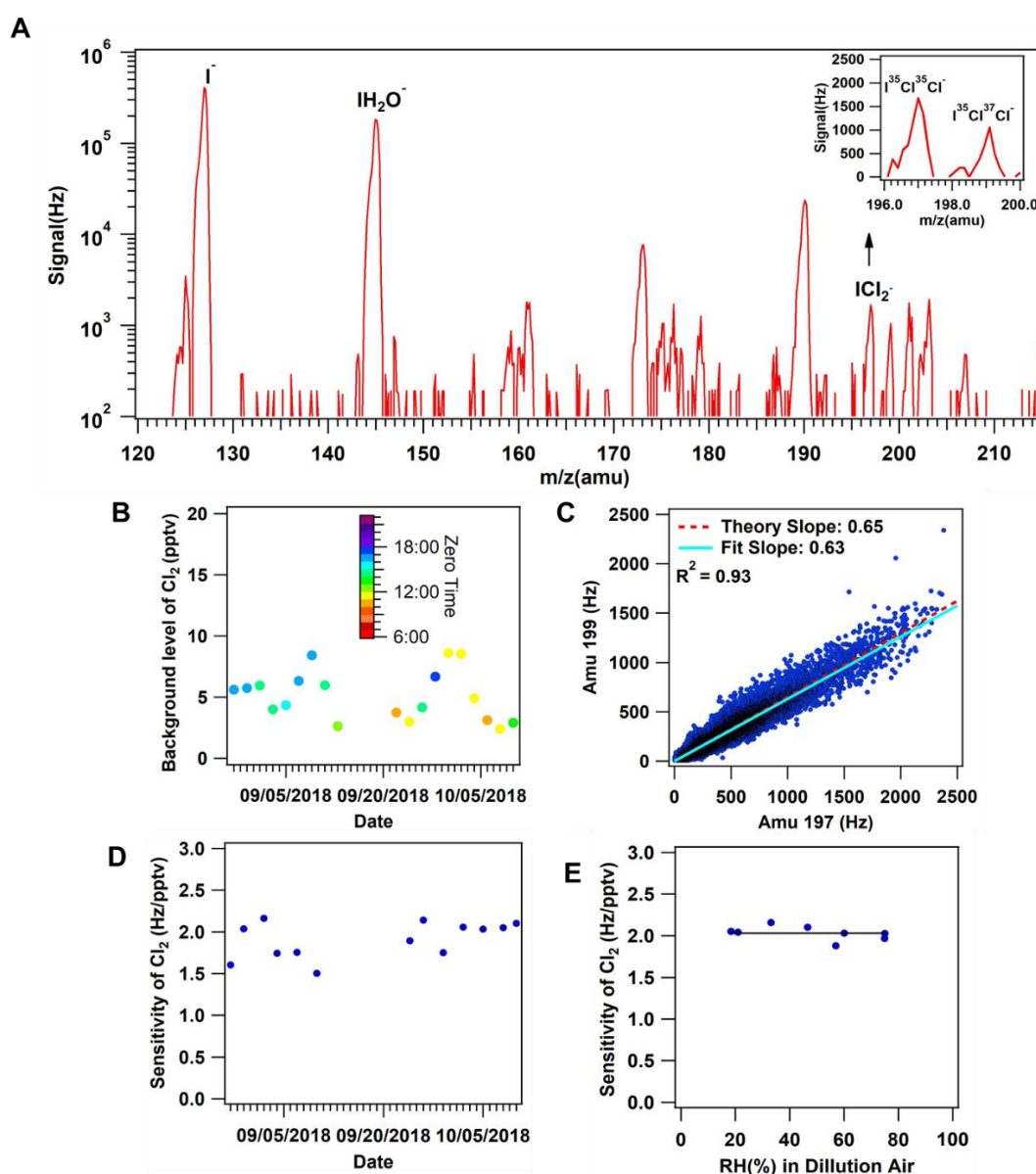
110 **Supplementary Fig. 13. Mean diurnal profile of Cl₂ and CMBO.** Besides the
111 inorganic chloride species, organochlorides (CLOVOCs) were also measured at the same
112 measurement site in Hong Kong using the High-Resolution Time of Flight Chemical
113 Ionization Mass Spectrometer (HR-ToF-CIMS) but at different period (14-26 November
114 2018). The detailed information of the instrument and identification of Cl-VOCs can be
115 found in the previous study ¹. Briefly, the HR-ToF-CIMS adopts chemical reactions to
116 ionize the target gases using iodide (I⁻) as the reagent ion. Along with Cl₂, thirteen
117 gas-phase C₁-C₆ CLOVOCs were detected, with 1-chloro-3-methyl-3-butene-2-one
118 (CMBO, C₅H₆ClO) as the most dominant organochloride. Cl₂ and CMBO were detected
119 as iodide adducts (ICl₂⁻ and IC₅H₆ClO⁻, respectively) after ion-molecule reactions: I⁻ +
120 Cl₂ → ICl₂⁻, I⁻ + C₅H₆ClO → IC₅H₆ClO⁻. Other species were measured with the similar
121 ionization chemistry. CMBO is the chlorine oxidation product of isoprene, which makes
122 this CLOVOC a unique tracer of chlorine-biogenic chemistry ^{2,3}. The daily maxima of
123 CMBO coincided with that of Cl₂, indicative of VOC oxidation by Cl atom. The color
124 region represents the standard deviation of the data set. This will be explained further in
125 succeeding studies. No calibration was conducted, and therefore the Cl₂ and CMBO
126 measurements shown here are in arbitrary units.



127



130 **Supplementary Fig. 14. The CIMS performance for Cl₂ ambient measurement from**
 131 **31 August to 9 October of 2018. (A)** An example of the mass spectrum of CIMS from
 132 120 amu to 220 amu during the field measurements. The signals below 10 Hz were not
 133 recorded during hourly scans but were recorded during measurements. The insert panels
 134 are the high-resolution scan spectra for Cl₂. **(B)** The background level of Cl₂ (the signal
 135 equivalent to concentration) during the campaign. **(C)** Scatter plot of the raw CIMS
 136 signal of Cl₂ at mass 199 amu (³⁵Cl³⁷Cl⁻; ³⁷Cl³⁵Cl⁻) versus 197 amu (³⁵Cl³⁵Cl⁻) with 10
 137 min average for the entire ambient measurement period. The blue lines are the measured
 138 ratios, and the red dashed lines are the theoretical isotopic ratios. **(D)** The sensitivity of
 139 Cl₂ was determined on-site to confirm the stability of CIMS. **(E)** The sensitivity of Cl₂
 140 under different RH in dilution zero air.



142 **Supplementary Tables:**

143 **Supplementary Table 1. Input parameters to the box model for halogen impact**
 144 **evaluation.** All listed parameters (except for CH₄ and HCHO) in the table were the
 145 concurrent measurement data at our site for period 4-14 September 2018. The VOCs
 146 names are given in MCM format.

No	Parameter	Time resolution	Average value ± Standard deviation
1	Temperature	1 min	27.7±1.25 °C
2	RH	1 min	82.8±4.42%
3	JNO ₂	1 min	0.0021±0.0026 s ⁻¹
4	NO	1 min	1.46±0.385 ppbv
5	NO ₂	1 min	4.45±1.53 ppbv
6	O ₃	1 min	55.4±14.0 ppbv
7	CO	1 min	260±10.2 ppbv
8	SO ₂	1 min	1.77±0.367 ppbv
9	N ₂ O ₅	1 min	0.051±0.051 ppbv
10	ClNO ₂	1 min	0.139±0.106 ppbv
11	Cl ₂	1 min	0.149±0.091 ppbv
12	HONO	1 min	0.238±0.0373 ppbv
13	C ₂ H ₆	1 min	1.21±0.209 ppbv
14	C ₂ H ₄	1 min	0.208±0.0472 ppbv
15	C ₃ H ₈	1 min	1.25±0.242 ppbv
16	C ₃ H ₆	1 min	0.102±0.0196 ppbv
17	IC ₄ H ₁₀	1 min	0.842±0.288 ppbv
18	NC ₄ H ₁₀	1 min	1.35±0.648 ppbv
19	TBUT ₂ ENE	1 min	0.627±0.153 ppbv
20	BUT ₁ ENE	1 min	0.0530±0.0106 ppbv
21	IC ₅ H ₁₂	1 min	0.529±0.130 ppbv
22	NC ₅ H ₁₂	1 min	0.448±0.065 ppbv
23	BENZENE	1 min	0.270±0.145 ppbv
25	TOLUENE	1 min	0.905±0.511 ppbv
26	CH ₃ CHO	1 min	1.141±0.865 ppbv
27	Cyclopentane	1 min	0.100±0.0284 ppbv
28	Methylcyclopentane	1 min	0.169±0.0509 ppbv
29	2,2,4-Trimethylpentane	1 min	0.0567±0.0134 ppbv
30	C ₅ H ₈	1 min	0.636±0.444 ppbv
31	C ₂ H ₅ CHO	1 min	0.289±0.0759 ppbv
32	CH ₃ COCH ₃	1 min	1.86±0.667 ppbv
33	M ₂₂ C ₄	1 min	0.0761±0.0194 ppbv
34	M ₂ PE	1 min	0.199±0.0694 ppbv

35	NC6H14	1 min	0.841±0.568 ppbv
36	C3H7CHO	1 min	1.283±0.364 ppbv
37	M2HEX	1 min	0.0485±0.0261 ppbv
38	CHEX	1 min	0.143±0.0593 ppbv
39	M3HEX	1 min	0.260±0.0449 ppbv
40	NC7H16	1 min	0.110±0.0413 ppbv
41	C5H11CHO	1 min	0.148±0.0210 ppbv
42	C5H4CHO	1 min	0.142±0.0296 ppbv
43	EBENZ	1 min	0.242±0.125 ppbv
44	PXYL	1 min	0.514±0.329 ppbv
45	OXYL	1 min	0.227±0.160 ppbv
46	BENZAL	1 min	0.0639±0.0075 ppbv
47	MXYLAL	1 min	1.35±0.80 ppbv
48	CH4	1 min	2000±0 ppbv
49	HCHO	1 min	3.34±0.275 ppbv

147

148

149 **Supplementary Table 2. The peak Cl₂ mixing ratios observed during illumination of**
150 **four ambient filter samples and corresponding aerosol composition.**

Filter Number	Cl ₂ Concentration	Cl ⁻ (μg m ⁻³) in Filter	NO ₃ ⁻ (μg m ⁻³) in Filter
01	300 pptv	8.66	5.95
02	550 pptv	10.59	2.90
03	Below detection limit	2.30	1.05
04	Below detection limit	0.57	0.72

151

152

153 **Supplementary Table 3. Instruments used in the field study.**

Measured Species	Instrumentation	Time Resolution
Cl ₂ , ClNO ₂ , N ₂ O ₅	Q-CIMS	1 min
* HONO	Q-CIMS	1 min
	LOPAP (QUMA, Model LOPAP-03)	10 min
NO, NO ₂	Chemiluminescence/photolytic converter (Thermo, Model 42i)	1 min
O ₃	UV photometric analyzer (Thermo, Model 49i)	1 min
** Compositions in PM _{2.5} and PM ₁₀ (including NO ₃ ⁻ , Cl ⁻ NH ₄ ⁺ , SO ₄ ²⁻)	MARGA	1 hour
Solar Radiation	Pyranometer (li-200, licor)	1 min
*** Dry-state particle number size distribution	WPS (model 1000XP, MSP Corporation)	
VOCs	GC-MS/FID (GC955 Series 611/811, Syntech Spectras)	1 hour
	off-line DNPH-Cartridge-HPLC	2 hours
	PTR-MS (PTR-QMS 500, IONICON Analytik, Austria)	10 min
OVOCs	off-line DNPH-Cartridge-HPLC	2 hours

154

155 * HONO was measured by CIMS and LOPAP in this study. The two instruments showed
 156 good agreement. The HONO data from the CIMS were used in model calculations.

157 ** The molar concentrations of inorganic ions (i.e., [Cl⁻], [NO₃⁻], and [H⁺]) in aerosol
 158 water were estimated using the extended aerosol inorganics model (E-AIM, model III) ^{4,5}
 159 (please see Methods section 2).

160 *** The dry-state particle number size distribution was measured by the WSP with a
 161 diffusion dryer, covering the size ranging from 10 nm to 10000 nm. The ambient (wet)
 162 particle number size distributions were calculated based on a size-resolved kappa-Köhler
 163 dependence on the relative humidity ⁶⁻⁹. The aerosol surface area density was calculated

164 with the wet ambient particle number size distribution assuming spherical particles. In the
165 present study, data with RH greater than 90 % were excluded due to the large uncertainty
166 of the growth factor at very high RH.

167

168 **Supplementary References**

- 169 1 Le Breton, M. *et al.* Chlorine oxidation of VOCs at a semi-rural site in Beijing:
170 significant chlorine liberation from ClNO₂ and subsequent gas- and particle-phase
171 Cl-VOC production. *Atmospheric Chemistry Physics* **18**, 13013-13030,
172 doi:10.5194/acp-18-13013-2018 (2018).
- 173 2 Nordmeyer, T. *et al.* Unique products of the reaction of isoprene with atomic chlorine:
174 Potential markers of chlorine atom chemistry. *Geophysical Research Letters* **24**,
175 1615-1618, doi:<https://doi.org/10.1029/97GL01547> (1997).
- 176 3 Tanaka, P. L. *et al.* Direct evidence for chlorine-enhanced urban ozone formation in
177 Houston, Texas. *Atmospheric Environment* **37**, 1393-1400,
178 doi:[https://doi.org/10.1016/S1352-2310\(02\)01007-5](https://doi.org/10.1016/S1352-2310(02)01007-5) (2003).
- 179 4 Wexler, A. S. & Clegg, S. L. Atmospheric aerosol models for systems including the ions
180 H⁺, NH₄⁺, Na⁺, SO₄²⁻, NO₃⁻, Cl⁻, Br⁻, and H₂O. *Journal of Geophysical Research:*
181 *Atmospheres* **107**, ACH 14-11-ACH 14-14 (2002).
- 182 5 Xia, M. *et al.* Significant production of ClNO₂ and possible source of Cl₂ from N₂O₅
183 uptake at a suburban site in eastern China. *Atmospheric Chemistry Physics* **20**, 6147-6158
184 (2020).
- 185 6 Liu, H. J. *et al.* Aerosol hygroscopicity derived from size-segregated chemical
186 composition and its parameterization in the North China Plain. *Atmospheric Chemistry*
187 *and Physics* **14**, 2525-2539, doi:10.5194/acp-14-2525-2014 (2014).
- 188 7 Hennig, T., Massling, A., Brechtel, F. J. & Wiedensohler, A. A Tandem DMA for highly
189 temperature-stabilized hygroscopic particle growth measurements between 90% and 98%
190 relative humidity. *Journal of Aerosol Science* **36**, 1210-1223,
191 doi:10.1016/j.jaerosci.2005.01.005 (2005).
- 192 8 Yu, C. *et al.* Heterogeneous N₂O₅ reactions on atmospheric aerosols at four Chinese sites:
193 improving model representation of uptake parameters. *Atmospheric Chemistry and*
194 *Physics* **20**, 4367-4378, doi:10.5194/acp-20-4367-2020 (2020).
- 195 9 Yun, H. *et al.* Nitrate formation from heterogeneous uptake of dinitrogen pentoxide
196 during a severe winter haze in southern China. *Atmospheric Chemistry and Physics* **18**,
197 17515-17527, doi:10.5194/acp-18-17515-2018 (2018).